Supporting Information

Reactive Chemical Vapor Deposition of heteroepitaxial $Ti_{1-x}Al_xN$ films

Frederic Mercier, Hiroyuki Shimoda, Sabine Lay, Michel Pons, Elisabeth Blanquet*

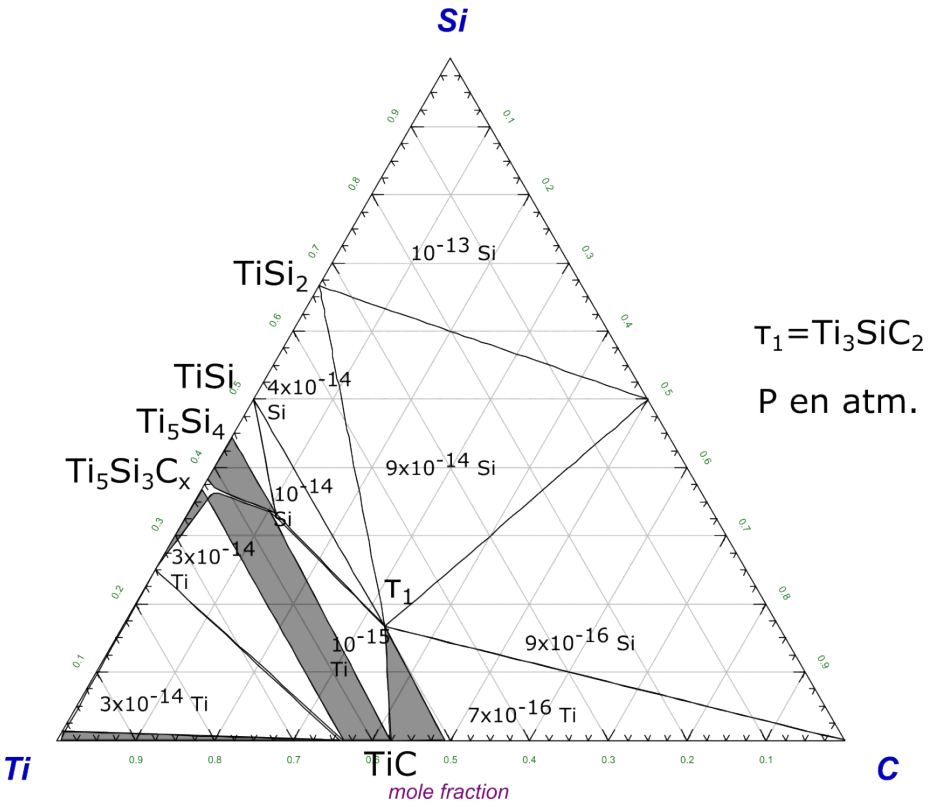

Figure S1. Calculated isothermal sections of the C-Si-Ti phase diagram at 900°C. Equilibrium pressures in the triphased domains are given in atm. The main constituent in the gas phase (Si or Ti) is also given.

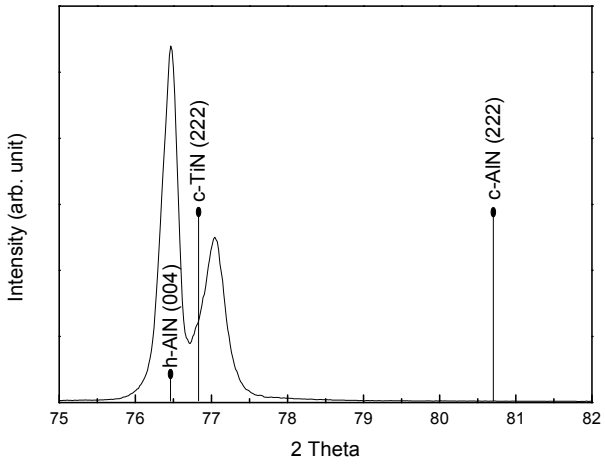

Figure S2. Typical X-ray diffraction pattern of the layer fabricated on monocrystalline AlN at 1200℃ showing the peaks of hexagonal AlN (004), cubic TiN (222) and cubic AlN (222).

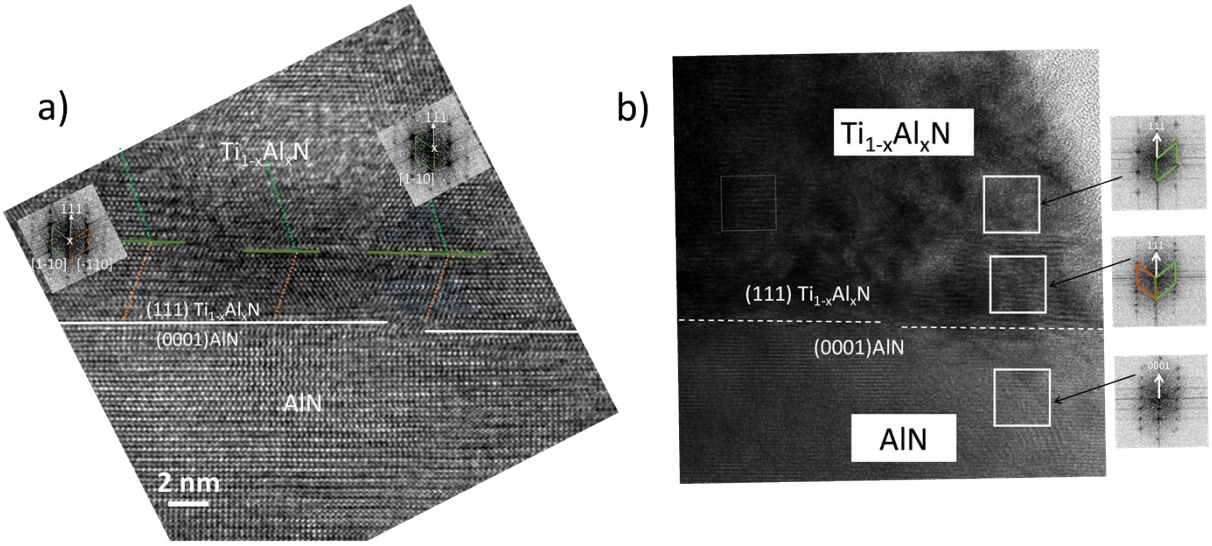

Figure S3. Two variants are observed in the layer as drawn in the layer. a) AlN viewed along [2-1-10] and $Ti_{1-x}Al_xN$ layer viewed along [-110]. The Fourier transform of the areas at the location of the inserts confirms the existence of two orientation variants of $Ti_{1-x}Al_xN$ with [1-10] and [-110] zone axis. b) Two variants of $Ti_{1-x}Al_xN$ viewed along [1-10] and [-110] directions in the thickness of the TEM thin foil.

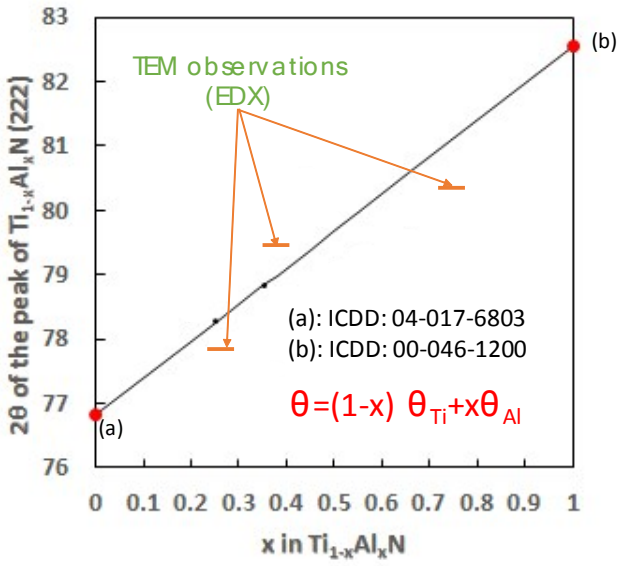

Figure S4. Determination of the Ti composition from the second order peak (222) of $Ti_{1-x}Al_xN$. The position of the (222) $Ti_{1-x}Al_xN$ reflection peak is located between the (222) peak of cubic TiN (ICDD: 04-017-6803) and the (222) peak of cubic AlN (ICDD: 00-046-1200). If no (or constant) mechanical constraints are considered in the $Ti_{1-x}Al_xN$ films, the observed shift is related to the value of x and its evolution is assumed to follow the Vegard's law. The Al content was also confirmed by EDX on three TEM samples prepared meaning that the mechanical stress component could be neglected in our experimental conditions.

Transport modeling

The governing equations describing flow dynamics, heat transfer and mass transport include continuity, momentum, energy and species balance (Table S1) The flow is laminar, obeys to the ideal gas law and steady-state conditions prevails. Precursors are very diluted in carried gas (more than 99% in mass of the gaseous phase) so values of the transport properties can be calculated by the kinetic theory of dilute gas [1].

Table S1. Governing equations of multicomponent mass transfer (notations given below)

Continuity	$\nabla \cdot \rho \vec{v} = 0$
Momentum balance (1)	$\nabla \cdot (\rho \vec{v}\vec{v}) = \nabla \cdot \underline{\underline{\tau}} - P + \rho \vec{g}$ $\underline{\underline{\tau}} = \mu\left(\nabla \vec{v} + (\nabla \vec{v})^t\right) - \frac{2}{3}\mu(\nabla \cdot \vec{v})\underline{\underline{I}}$
Energy balance (2)	$c_p \nabla \cdot (\rho \vec{v} T) = \nabla \cdot (\lambda \nabla T) + \nabla \cdot \left(RT \sum_{i=1}^{N} \frac{D_i^T}{M_i} \frac{\nabla x_i}{x_i} \right)$ $+ \sum_{i=1}^{N} \frac{H_i}{M_i} \nabla \cdot \vec{J}_i - \sum_{i=1}^{N} \sum_{k=1}^{K} H_i \upsilon_{ik} \left(R_k^g - R_{-k}^g \right)$
Species transport (3)	$\nabla \cdot (\rho \vec{v} \omega_i) = -\nabla \cdot \vec{J}_i + M_i \sum_{k=1}^{K} \upsilon_{ik} \left(R_k^g - R_{-k}^g \right)$ $i = 1, N$ $\vec{J}_i^c = -\sum_{j=1}^{N} (\rho D_{ij}) \nabla x_j \quad i = 1, N$ $\vec{J}_i^T = -D_i^T \frac{\nabla T}{T} \quad i = 1, N$
Ideal gas law (4)	$\rho = \frac{PM}{RT}$
Deposition rate (5)	$R_s = \vec{J}_i . \vec{n} = \vec{J}_i^c . \vec{n} + \vec{J}_i^T . \vec{n} \quad i = 1, N$

The boundary conditions for velocity, temperature and species concentration are the following. The temperature and concentration distribution are uniform at the inlet of the tube. A zero gradient in concentration is fixed at all non-reactive surfaces. On reactive surfaces, equation (5) is applied. The pressure at the inlet is varied such that the calculated flow rates in the outlet match the experimental conditions. The temperature of the reactor walls is specified from measurements. The properties of the individual species and binary diffusion coefficients are estimated using gas kinetic theory [1].

Kinetics pathways for titanium deposition from $TiCl_4 + H_2$

The appearance of the different chlorides of titanium in the temperature range 1000-1800 K in flowing hydrogen was calculated by the minimization of the Gibbs free energy of the Ti-Cl-H system. The database used is Scientific Group Thermodata Europe (SGTE). The main specie coming out the evaporation chamber is $TiCl_4$. In all systems involving a transition metal, there

is a progressive evolution of the precursor to lower oxidation states [2-4]. Any titanium chlorides could be reactive on the surface. The kinetic model involves both homogeneous gas-phase and heterogeneous surface reactions. The basic gas-phase mechanism of $TiCl_4$ decomposition is summarized in the paper of Teyssandier et al. [2] (Table S2). The homogeneous gas phase reactions are tied to the unimolecular decomposition of $TiCl_4$ for evaporation systems.

Initiation :	$TiCl_4 <-> TiCl_3 + Cl$	(G1)
Cl/H partial equilibrium:	$Cl + H_2 <-> HCl + H$	(G2)
$TiCl_3$ production:	$TiCl_4 + H <-> TiCl_3 + HCl$	(G3)
$TiCl_2$ production (low pressure):	$TiCl_3 + H <-> TiCl_2 + HCl$	(G4)
TiCl production (high pressure):	$TiCl_3 <-> TiCl + Cl$	(G5)

Table S2. Rate coefficients expressed as $AT^n \exp(—E/RT)$. For unimolecular reactions, the units of A are s^{-1}; for bimolecular reactions the units are $cm^3\ mol^{-1}$; all energies are in $kJ.mol^{-1}$.

Reaction	A	n	E
G1	2.32 E+20	-1.17	387.9
G2	2.95E+13	0	21.3
G3	5.11E+6	2.5	12.6
G4	1.11E+6	2.5	33.5
G5	1.02E18	-0.742	422.6

At high temperature (1500 K at $P=10^5$ Pa), the equilibrium regime is rapidly reached and more than 10 % of the input $TiCl_4$ is converted to lower chlorides. For lower temperatures (1000 K), the equilibrium regime requires much longer times (> 300 s) than the typical residence time in the experiments. $TiCl_4$ is practically not decomposed by homogeneous reactions.

Surface reactions are implemented such as all chlorides can react to form solid titanium. The reactions are written as first order kinetics. $TiCl_m$ (m=1, 4) species are adsorbed on available sites <s> and react with different probabilities to give Ti(S). Only the adsorption of the gaseous species $TiCl_m$ (m=1, 4) are important for the development of the heterogeneous kinetic mechanism.

$TiCl_m$ +<s> <-> Ti (S) + mCl (S)

The Gibbs free energy of these heterogeneous reactions decreases from 200 kJ to 50 kJ at 1300 K when y decreases from 4 to 2. The reaction probability of titanium chlorides increases when y decreases. It was assumed a low sticking coefficient for $TiCl_4$ (10^{-3}) and higher sticking coefficients for $TiCl_3$ (0.1) $TiCl_2$ (0.5) and TiCl (1). From these values, the Arrhenius form of data were evaluated [5-6] and the gas-solid mechanisms are summarized in Table S3.

Table S3. Rate coefficients expressed as AT^n exp(—E/RT). (SI units, m, kg, s)

Reaction	A	n	Ea/R (K)
S1 (y=4)	1.6 E2	0.5	7700
S2 (y=3)	2.1 E4	0.5	8200
S3 (y=2)	2 E5	0.5	8200
S4 (y=1)	3E6	0.5	8200
Site density	1.8E-5 mol/m²		

The transport properties of the mixture, conductivity, viscosity, specific heat, and diffusion coefficients are estimated by the kinetic theory of dilute gas [1]. Table S4 summarizes the Lennard-Jones parameters used for the calculation. Thermodynamic data were found in the Chemkin thermodynamic database [7] and are fitted by polynomials.

Table S4. Lennard-Jones parameters for the estimation of transport properties

Species Name	Mol Wt (g/mol).	Coll. Dia.(A)	Energy (K)
HCl	3.65E+01	3.34E+00	3.45E+02
H2	2.02E+00	2.83E+00	5.97E+01
TiCl4	1.90E+02	4.98E+00	2.67E+02
TiCl3	1.54E+02	4.98E+00	2.67E+02
TiCl2	1.19E+02	4.98E+00	2.67E+02
Cl	3.55E+01	3.61E+00	1.31E+02
H	1.01E+00	2.71E+00	3.70E+01
Cl2	7.09E+01	4.22E+00	3.16E+02

Main results

The flow is laminar without any buoyancy effects in the experimental conditions used (Figure S5) : Flow rate of H_2 = 1SLM (standard litre per minute), flow rate of reactive species = 2 SCCM (standard cubic centimeter per minute), temperature of the susceptor varying from 1000 to 1800 K, Pressure = 1000 Pa. When the temperature increases, $TiCl_4$ is more and more transformed in lower chorides (Figure S6 and S7). At the highest temperature studied (1800 K), its mole fraction at the surface is near zero. $TiCl_2$ species appears only at high temperature in the hot regions and is consumed on the substrate surface (Figure S6 and S7).

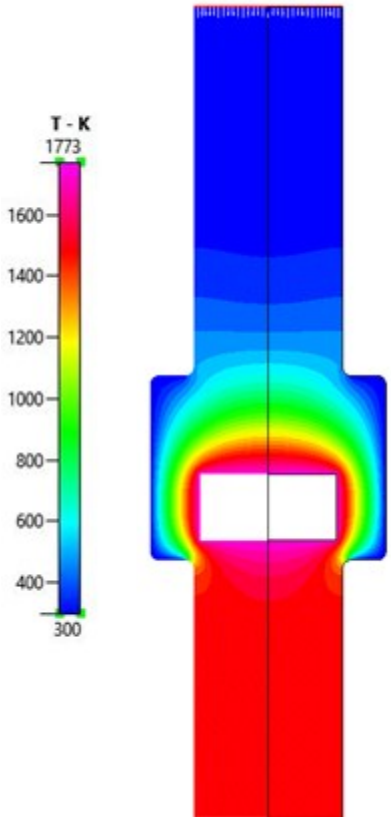

Figure S5. Temperature field

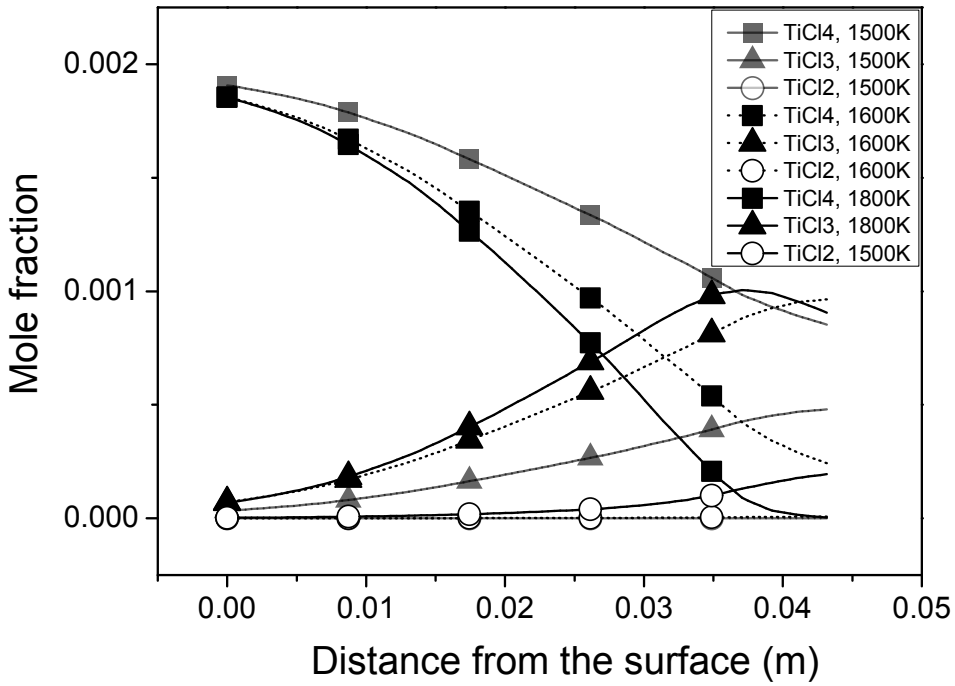

Figure S6. Evolution of chlorides mole fraction above the substrate as a function of temperature. The flow rate of H_2 is 1 SLM and the initial mole fraction of $TiCl_4$ at the entrance of the reactor is 0.2 %.

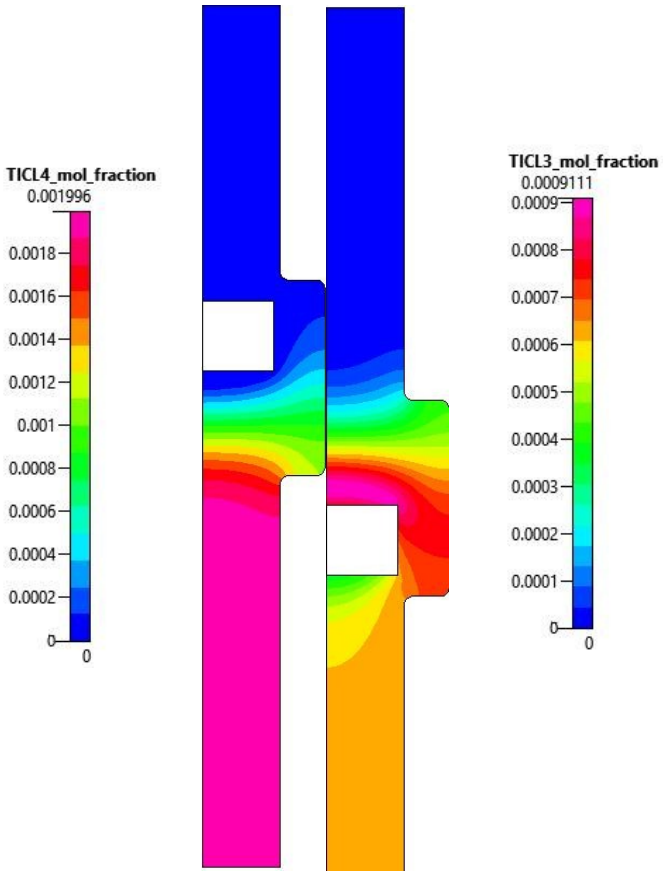

Figure S7. Mole fraction fields of $TiCl_4$ and $TiCl_3$ (conditions of figure 2 at T=1800 K)

Ti diffusion and reaction on AlN

The titanium flux at the surface is determined by the surface reaction (S1-S4). Titanium is not only a solute in the AlN phase but it is participating to its structure (hexagonal to cubic solid solution). The driven force for diffusion is not the concentration gradient but the activity gradient:

$$J_{Ti} = -\rho D_{Ti} \frac{da}{dx}$$

The a are the activity coefficients of Ti in TiAlN close to the surface and in the gas-phase. D is the so-called mass-transfer coefficient and may depend on both temperature and gas composition. The activity of Ti in the gas-phase depends on the balance of reactions (Table S2 and S3), heat transfer and fluid mechanics.

Initial conditions are: t=0, x>0, $c(x,0)=c_0$

Boundary conditions are: $t>0$, $x=0$, $c(0,t)=c_{surface}$

The titanium flux at the surface is determined by the surface reactions (S1-S4). There is a rapid diffusion of deposited titanium into the AlN thin layer (1 μm). The diffusion of Ti in the AlN layer leads to a complex mechanism of interdiffusion. The driven force for diffusion is the activity gradient. For the kinetic simulations, a model for long range diffusion occurring in a continuous matrix was used. It was assumed that diffusion occurs only in the AlN thin film. This assumption is based on the fact that the diffusion of Ti leads to a supersaturated solid solution with AlN. The growth kinetics for fcc-$Ti_{1-x}Al_xN$ phase formation can be regarded as a diffusion-controlled reaction. For the description of the flux of species driven by a concentration gradient, the multi-component diffusion theory was applied. The titanium in-diffusion is driven by concentration gradients in the AlN thin film. There are no data on the diffusion of titanium through AlN thin films leading to a metastable solid solution. However, Imanaka et al. [8] performed reactive diffusion of thin Ti films deposited on AlN to form titanium aluminides. The activation energy (224 kJ/mol) is very similar to that for nitrogen diffusion in titanium (220 kJ/mol). The diffusion coefficient values are very similar to that for W diffusion in AlN [9].

Assuming the formation of a solid solution and the value of the diffusion coefficient calculated by Imanaka et al. [8], there is a good agreement between the thickness of the transformed zones and titanium diffusion length in AlN when the temperature is higher than 1150 K (Figure 2). This temperature is the onset of an equilibrium regime between deposition flux and diffusion flux. For lower temperatures, the deposition rate is too low and diffusion rate is higher than deposition rate. There is not enough material on the surface to compensate Ti diffusion. It is worth noting that the diffusivities found are very low and indicate a very slow diffusion of titanium atoms through AlN layers. The mean penetration at 1200 K does not exceed 40 nm after 1h.

References for the Supporting Information

[1] R.B. Bird, W.E. Stewart, E.N. Lightfoot, Transport phenomena, John Wiley &Sons, NY, **1960**.

[2] F. Teyssandier, M.D. Allendorf,, J. Electrochem. Soc. **1998**, 145, 2167.

[3] J.A. Atwoki, S. Eriksen, I. Petrushina, E. Christensien, N.J. Bjerrum, Adv. Mater. Interfaces **2016**, 1500795

[4] J. Herzler, P. Roth, Proc. Combust. Inst **2002**, 29, 1353.

[5] P.J Van de Put, J.A.M. Ammerlaan, J.P. Dekker, J. Schoonman, Chem. Vap. Deposition **1999**, 5, 211.

[6] R. Boichot, N. Coudurier, F. Mercier, A. Claudel, N. Baccar, A. Milet, E. Blanquet, M. Pons, Theor. Chem. Acc. **2014**, 133, 1419.

[7] R.J. Kee, F.M. Rupley, J.A. Miller, Sandia report **1990,** SAND87-821B.

[8] Y. Imanaka, M. R. Notis, J. Am. Ceram. Soc. **1999**, 82, 1547.

[9] X. He, S.Z. Yang, K. Tao, Y. Fan, Mater. Lett. **1997** 33, 175.

Notations and units

R_S	:	surface reaction rate ($kg.m^{-2}.s^{-1}$)
$\underline{v}$	:	velocity vector ($m.s^{-1}$)
P	:	pressure (Pa)
x_i	:	species molar fraction of species i
ω_i	:	species mass fraction of species i
T	:	temperature (K)
$\underline{g}$	:	gravity vector ($g = 9.81\ m.s^{-2}$)
I	:	unity tensor
R	:	universal gas constant ($8.314\ J.mol^{-1}.K^{-1}$)
M	:	molar mass of the mixture ($kg.mol^{-1}$)
N	:	number of gaseous species in the mixture
ρ	:	density ($kg.m^{-3}$)
λ	:	thermal conductivity of the gas mixture ($W.m^{-1}.K^{-1}$)
μ	:	dynamic viscosity of the gas mixture ($kg.m^{-1}.s^{-1}$)
C_p	:	specific heat of the gas mixture ($J.kg^{-1}.K^{-1}$)
$\underline{n}$	:	unity vector normal
ρ	:	density (kg.m-3)
h	:	advection coefficient ($W.m^{-2}.K^{-1}$)

T_{amb}	:	ambient temperature (K)
σ_{st}	:	Stefan-Boltzmann constant ($W.m^{-1}.K^{-4}$)
ε	:	emissivity
$\mathbf{n}$	:	unity vector normal to the wall
$\Re_{gi}$	:	reaction rate of reaction i in the gas phase ($kg.m^{-3}.s^{-1}$)
$\mathbf{J}_i^F$	:	diffusive mass flux vector ($kg.m^{-2}.s^{-1}$)
$\mathbf{J}_i^T$	:	thermo-diffusive mass flux vector ($kg.m^{-2}.s^{-1}$)
D_{ij}	:	multicomponent diffusion coefficients ($m^{-2}.s^{-1}$)
D_i^T	:	multicomponent thermodiffusion coefficients ($kg.\ m^{-1}.s^{-1}$)